AUT Journal of Electrical Engineering
10.22060/EEJ.2026.25565.5962

Backstepping control of Quanser's 2-DOF Helicopter under disturbance and actuator saturation based on Flower Pollination Algorithm

Imam Barket Ghiloubi[1,*], Latifa Abdou[2]

[1]PhD candidate, Identification Command Control & Communication Laboratory, Faculty of Sciences and Technology, Mohamed Khider University, Biskra, Algeria

Corresponding author email: imam.ghiloubi@univ-biskra.dz

[2]Professor, Department of Electronics, Mustapha Ben Boulaïd University, Batna, Algeria

Abstract:

This paper presents a robust backstepping control strategy for Quanser's 2-Degree-of-Freedom (2-DOF) helicopter, addressing challenges posed by external disturbances and actuator saturation constraints. The proposed approach leverages Flower Pollination Algorithm (FPA) to fine-tune the control parameters, enhancing system stability and performance. Initially, a mathematical model of the 2-DOF helicopter is derived, incorporating non-linear dynamics and actuator limits. The backstepping control framework is then developed, integrating disturbance rejection mechanisms to mitigate external perturbations. FPA is employed to optimize the controller gains, ensuring optimal performance under various operational scenarios. Extensive simulation results demonstrate the effectiveness of the proposed method, displaying significant improvements in tracking accuracy and robustness against disturbances and actuator saturation compared to conventional control techniques. This study shows the potential of combining the proposed metaheuristic optimization algorithm with robust control strategy for complex aerospace systems like helicopter.

Keywords:

Nonlinear control, Aerial robotics, Optimization, Disturbance, Robustness.

1. Introduction

Controlling a two-degree-of-freedom (2-DOF) helicopter is a fascinating challenge that combines theory and practice in the aerospace field. This type of system, often used in research and training environments, allows researchers to explore advanced concepts in dynamics and control. The motivation for mastering 2-DOF helicopter control lies in the need to understand and optimize the complex interactions between the controls and the dynamic response of the aircraft. By refining these skills, engineers and researchers can develop more robust and accurate control techniques, contributing to the advancement of aeronautical technologies and the realization of more sophisticated control systems for diverse applications ranging from simulation to aerial robotics. An adaptive neural network tracking control scheme for MIMO nonlinear systems with quantized input saturation is developed achieving stable and effective tracking as shown in simulations and experiments on a two-degree-of-freedom helicopter system [1]. A novel adaptive neural network-based, fault-tolerant control scheme for a two-degree-of-freedom helicopter system is proposed and validated in [2] to address issues of uncertainty, unknown control direction, and actuator faults. A study on a model-free LQR based PID controller for tracking control in a 2-DoF laboratory helicopter is presented in paper [3], with the goal of improving trajectory tracking of pitch and yaw axes despite disturbances and the nonlinear character of the system. For the control problem of the Twin Rotor MIMO System (TRMS), two fuzzy logic PID controllers are developed. The performance of a model-free LQR based PID controller created for the tracking control problem of a 2-DoF lab helicopter is proposed and evaluated in [4]. An adaptive neural control with time-varying output constraints and input saturation for uncertain 2DOF helicopter systems is developed [5]. A Nonlinear Model Predictive Control (NMPC) to regulate TRMS and Fick's Law Algorithm (FLA) has been applied to find the ideal choice for NMPC settings offline [6]. A trajectory tracking control strategy for a 2-DOF helicopter is proposed by [7] using a gradient descent-based learning control law to minimize the error dynamics as an objective function. Another paper presents a nonlinear PID control method based on a modified sorting

10.22060/EEJ.2026.25565.5962

genetic algorithm that has been verified using the laboratory helicopter model, Twin Rotor System [8]. A hybrid control method combines nonsingular terminal sliding mode (NTSM) control, metaheuristic optimization algorithms and adaptive super-twisting technique to control the Quanser aero simulator helicopter [9]. In [10], the authors present the modeling and control of a laboratory 2-DOF MIMO helicopter based on an Euler–Lagrange formulation, where a fuzzy-tuned PID controller is shown to outperform the conventional PID in terms of stability and control performance through simulation and experimental results.. Through theoretical research and real-world tests, the Extended Kalman Filter (EKF)'s capacity to estimate the state of a MIMO twin rotor system is explored and shown [11]. Paper [12] discusses the challenges involved in developing tracking control for twin rotor systems. Specifically, it highlights two main issues: the absence of a mathematical model for the twin rotor system and the lack of available measurements for angular velocity, both of which complicate the control problem. An embedded controller serves as the foundation for the real-time multivariable adaptive robust control proposed in [13] using an eigen structure assignment approach for its state space construction, the developed controller is assessed over a twin rotor MIMO system. A trajectory tracking control scheme for a 2-DOF helicopter is proposed based on feedback linearization combined with a GPI controller, where a convolutional neural network is employed to estimate unmeasured angular velocity and viscous friction, ensuring robust performance under disturbances. [14]. The control technique proposed in [15] is a robust generalized dynamic inversion based adaptive recursive sliding mode control (RGDI-ARSMC).A review of various published control algorithms for the control of a twin rotor aerodynamical system (TRAS) and twin rotor MIMO system (TRMS) is presented in [16]. Article [17] introduces a passive fault-tolerant controller leveraging robust techniques to fine-tune a proportional-derivative scheme via a linear matrix inequality. In order to stabilize a twin-rotor helicopter model and enhance its capacity to effectively reject external disturbances, an experimental examination into the efficacy of a novel hybrid control system is developed based on an intelligent active force control (IAFC) strategy [18]. In [19], a unique robust optimal control law for continuous variable perturbations in the Twin Rotor MIMO System (TRMS) is designed and enhanced with Robust Generalized Dynamic Inversion (RGDI). Paper [20] presents a novel mixed-optimization framework based on the Method of Inequality (MOI) and H1 model for uncertain Multi Input Multi Output (MIMO) systems, with a particular focus on UAVs. Important issues including unmodeled dynamics, noise interference, and parameter fluctuations are adaptively addressed by the suggested method. In [21], a vision-based UAV target-tracking approach is developed in GPS-denied environments using a cascaded adaptive nonlinear Model Predictive Control (MPC) scheme. An Extended Kalman Filter (EKF) is used to estimate uncertain model parameters, while the control law is parameterized to reduce computational cost and enable real-time implementation. Experimental results on a 2-DoF helicopter show effective and accurate target tracking under dynamic constraints. By using a mathematical study based on Lyapunov stability and taking into account disturbances, the strategy designed in [22] seeks to increase robustness of Unmanned Aerial Vehicle UAV and it is applied on the TRMS helicopter. To provide a clearer overview of existing control strategies applied to helicopter and similar nonlinear systems, a comparative summary of relevant literature is presented in Table 1. This table highlights the differences between control approaches in terms of methodology, optimization techniques, robustness, and system type.

Table 1. Obtained controller gains

Reference	Control Method	Optimization	Platform	Disturbance Handling	Limitation
PID-based works	PID	None	TRMS/ Helicopter	Weak	Poor robustness
Backstepping approaches	Nonlinear Backstepping	Manual tuning	2-DOF Helicopter	Moderate	No optimal tuning
LQR methods	Optimal control	Riccati	UAV/ Helicopter	Medium	Linear assumption
Metaheuristic methods	GA/PSO/ GWO	Evolutionary	UAV systems	Good	High computational cost

10.22060/EEJ.2026.25565.5962

Proposed method	Backstepping + FPA	Flower Pollination Algorithm	2-DOF Helicopter	Strong	Nonlinear + saturated system

The main contribution of this work lies in the integration of a nonlinear backstepping control strategy with an evolutionary optimization technique (Flower Pollination Algorithm) for the tuning of controller gains of a 2-DOF Quanser helicopter under external disturbances and actuator saturation constraints. Unlike classical backstepping or PID-based approaches commonly reported in the literature, the proposed method does not rely on fixed or manually tuned gains, but instead employs a simulation-based optimization framework to automatically determine optimal parameters that minimize the tracking error. Furthermore, the proposed approach ensures improved transient performance and robustness through the combination of nonlinear control design and global optimization capability of the FPA. The structure of this paper is as follows: Section 2 provides the mathematical model of the 2-DOF helicopter and then the nonlinear state space. Section 3 outlines the design of the backstepping control strategy of each angular position Pitch and Yaw. Section 4 introduces the Flower Pollination Algorithm FPA and its application in tuning the controller parameters. Section 5 presents the simulation results, demonstrating the effectiveness and robustness of the proposed approach. By combining backstepping control with the Flower Pollination Algorithm, this study aims to contribute to the field of control systems by providing a robust solution for managing complex aerospace systems under challenging conditions such as external disturbances.

2. Mathematical modeling

Quanser's 2DOF helicopter is an electromechanical system consisting mainly of a symmetric body, 2 position sensors and 2 motors that simulate the movement of a real helicopter to carry out control tests in the laboratory (Figure 1).

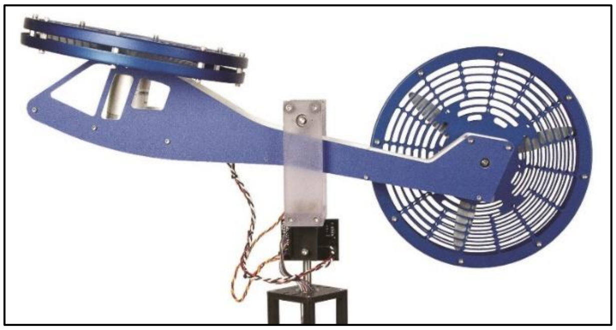

Fig. 2. Quanser's 2-DOF laboratory Helicopter

The studied system is a flying robot with two degrees of freedom, represented by the angular displacements theta θ (around the pitch axis) and psi ψ (around the yaw axis) (Figure 02).

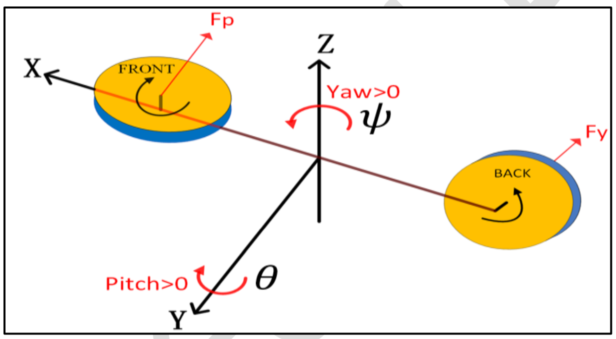

Fig. 2. Projection of Quanser's 2-DOF helicopter on a real helicopter

The mathematical model can be written as follows by calculating the accelerations around the two axes pitch and yaw with two control voltages V_p and V_y to operate the two motors of the system:

$$\ddot{\theta} = \frac{-mLgcos\theta - D_{pp}\dot{\theta} - mL^2\dot{\psi}^2 sin\theta cos\theta + k_{pp}V_p + k_{py}V_y}{mL^2 + I_{pp}} \tag{1}$$

$$\ddot{\psi} = \frac{-D_{yy}\dot{\psi} + 2mL^2\dot{\theta}\dot{\psi} sin\theta cos\theta + k_{yp}V_p + k_{yy}V_y}{mL^2(cos\theta)^2 + I_{yy}} \tag{2}$$

In this paper, helicopter's mathematical model is written in another way by changing the control part with the control signals U_1 and U_2 to be able to develop a non-linear controller calculating control laws passing to the robot through these two signals.

10.22060/EEJ.2026.25565.5962

$$\ddot{\theta} = \frac{-mLgcos\theta - D_{pp}\dot{\theta} - mL^2\dot{\psi}^2 sin\theta cos\theta}{mL^2 + I_{pp}} + \frac{1}{mL^2 + I_{pp}}U_1 \tag{3}$$

$$\ddot{\psi} = \frac{-D_{yy}\dot{\psi} + 2mL^2\dot{\theta}\dot{\psi}sin\theta cos\theta}{mL^2(cos\theta)^2 + I_{yy}} + \frac{1}{mL^2(cos\theta)^2 + I_{yy}}U_2 \tag{4}$$

Such as :

$$U_1 = k_{pp}V_p + k_{py}V_y \tag{5}$$

$$U_2 = k_{yp}V_p + k_{yy}V_y \tag{6}$$

Using equations (3) and (4), a nonlinear state space model is concluded to be used in the development of a nonlinear controller based on the backstepping method.

$$\dot{x}_1 = x_2 \tag{7}$$

$$\dot{x}_2 = \frac{-mLgcos\theta - D_{pp}\dot{\theta} - mL^2\dot{\psi}^2 sin\theta cos\theta}{mL^2 + I_{pp}} + \frac{1}{mL^2 + I_{pp}}U_1 \tag{8}$$

$$\dot{x}_3 = x_4 \tag{9}$$

$$\dot{x}_4 = \frac{-D_{yy}\dot{\psi} + 2mL^2\dot{\theta}\dot{\psi}sin\theta cos\theta}{mL^2(cos\theta)^2 + I_{yy}} + \frac{1}{mL^2(cos\theta)^2 + I_{yy}}U_2 \tag{10}$$

State variable vector is:

$$[x_1 \quad x_2 \quad x_3 \quad x_4]^T = [\theta \quad \dot{\theta} \quad \psi \quad \dot{\psi}]^T \tag{11}$$

3. Helicopter's nonlinear control

A backstepping controller is developed from nonlinear state space model of Quanser's helicopter and optimized using Flower Pollination Algorithm metaheuristic technique (FPA) to be tested under external disturbances.

Taking the first subsystem from equations (7) and (8) describing angular movement θ which is the variable x_1:

The position error is expressed by:

10.22060/EEJ.2026.25565.5962

$$\xi_1 = x_{1d} - x_1 \tag{12}$$

It is necessary to choose a Lyapunov function making this error ξ_1 converge to 0.

$$h(\xi_1) = \frac{1}{2}{\xi_1}^2 \tag{13}$$

Then, the derivative is:

$$\dot{h}(\xi_1) = \xi_1\dot{\xi}_1 = \xi_1(\dot{x}_{1d} - \dot{x}_1) \tag{14}$$

Substituting equation (7) into equation (14) gives:

$$\dot{h}(\xi_1) = \xi_1\dot{\xi}_1 = \xi_1(\dot{x}_{1d} - x_2) \tag{15}$$

A desired expression to follow x_{2d} must be developed to control the variable x_2, and this to guarantee that the function of equation (15) is negative semi-definite to complete the Lyapunov stability condition.

$$x_{2d} = \dot{x}_{1d} + \mu_1\xi_1 \quad , \quad \forall\mu_1 > 0 \tag{16}$$

The error of second state variable is expressed by:

$$\xi_2 = x_{2d} - x_2 \tag{17}$$

Another Lyapunov function depending on ξ_1 and ξ_2 is chosen as:

$$\mathcal{M}(\xi_1, \xi_2) = \frac{1}{2}({\xi_1}^2 + {\xi_2}^2) \tag{18}$$

Its derivative is:

$$\dot{\mathcal{M}}(\xi_1, \xi_2) = \xi_1\dot{\xi}_1 + \xi_2\dot{\xi}_2 \tag{19}$$

x_{2d} in equation (17) is replaced by equation (16):

$$\xi_2 = \dot{x}_{1d} + \mu_1\xi_1 - x_2 \quad , \quad \forall\mu_1 > 0 \tag{20}$$

Using equation (17), the second error ξ_2 can be written as follows:

$$\xi_2 = \dot{\xi}_1 + \mu_1\xi_1 \quad , \quad \forall\mu_1 > 0 \tag{21}$$

So:

$$\dot{\xi}_1 = \xi_2 - \mu_1\xi_1 \quad , \quad \forall\mu_1 > 0 \tag{22}$$

And $\dot{\xi}_2$ can be calculated from equation (20):

$$\dot{\xi}_2 = \ddot{x}_{1d} + \mu_1\dot{\xi}_1 - \dot{x}_2 \quad , \quad \forall\mu_1 > 0 \tag{23}$$

As a final step before developing control law, equation (19) should be written as follows to calculate the control law:

$$\dot{\mathcal{M}}(\xi_1,\xi_2) = \xi_1(\xi_2 - \mu_1\xi_1) + \xi_2\left(\ddot{x}_{1d} + \mu_1\dot{\xi}_1 - \dot{x}_2\right) \quad , \quad \forall\mu_1 > 0 \tag{24}$$

$\dot{x}_2$ is replaced by its expression mentioned in the equation (8):

$$\dot{\mathcal{M}}(\xi_1,\xi_2) = \xi_1(\xi_2 - \mu_1\xi_1) + \xi_2\left(\ddot{x}_{1d} + \mu_1\dot{\xi}_1 - \frac{-mLgcos\theta - D_{pp}\dot{\theta} - mL^2\dot{\psi}^2sin\theta cos\theta}{mL^2 + I_{pp}} - \frac{1}{mL^2 + I_{pp}}U_1\right), \forall\mu_1 > 0 \tag{25}$$

To satisfy the stability condition according to Lyapunov's theorem, the function of equation (25) must be negative semi-definite, which requires the choice of a control law U_1 which ensures that $\dot{\mathcal{M}}(\xi_1,\xi_2)$ be negative semi-definite:

$$U_1 = \left(mL^2 + I_{pp}\right)\left(\ddot{x}_{1d} + \mu_1\dot{\xi}_1 + \xi_1 + \mu_2\xi_2\right) + mgLcos\theta + D_{pp}\dot{\theta} + mL^2\dot{\psi}^2sin\theta cos\theta\,, \ \forall\mu_1 > 0\,, \forall\mu_2 > 0 \tag{26}$$

After substituting the control law U_1 into Equation (25), the derivative of the Lyapunov function becomes negative definite for all $\mu_1 > 0$ and $\mu_2 > 0$. Therefore, according to Lyapunov stability theory, the tracking errors ξ_1 and ξ_2 asymptotically converge to zero, which guarantees the asymptotic stability of the pitch subsystem.

Control law U_2 is concluded by taking the second subsystem from equations (9) and (10) describing angular movement ψ which is the variable x_3 and following the same previous steps of backstepping.

$$U_2 = \left(mL^2(cos\theta)^2 + I_{yy}\right)\left(\ddot{x}_{3d} + \mu_3\dot{\xi}_3 + \xi_3 + \mu_4\xi_4\right) + D_{yy}\dot{\psi} - 2mL^2\dot{\theta}\dot{\psi}sin\theta cos\theta\,, \ \forall\mu_3 > 0\,, \forall\mu_4 > 0 \tag{27}$$

Following the same backstepping design procedure for the yaw subsystem, the derivative of the corresponding Lyapunov function is also negative definite for all $\mu_3 > 0$ and $\mu_4 > 0$. Consequently, the tracking errors ξ3\xi_3ξ3 and ξ4\xi_4ξ4 asymptotically converge to zero, ensuring the asymptotic stability of the yaw subsystem.

According to the helicopter's nonlinear model presented in equations (1) and (2), the voltages V_p and V_y are the real input signals to be calculated, therefore formulas are extracted from equations (5) and (6) and written as function of the control laws U_1 and U_2 to calculate the corresponding voltages:

$$V_p = \frac{U_1 - \frac{k_{py}U_2}{k_{yy}}}{k_{pp} - \frac{k_{yp}k_{py}}{k_{yy}}} \tag{28}$$

$$V_y = \frac{U_2 - \frac{k_{yp}U_1}{k_{pp}}}{k_{yy} - \frac{k_{py}k_{yp}}{k_{pp}}} \tag{29}$$

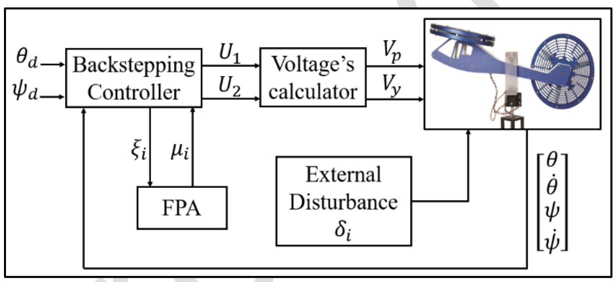

Fig. 3. General diagram of proposed control method

Figure 3 shows the general schematic of the proposed controller applied to the helicopter under external disturbances.

Backstepping controller uses desired angular positions θ_d and ψ_d with θ, ψ, $\dot{\theta}$, $\dot{\psi}$, to calculate control laws U_1 and U_2 and then control inputs V_p and V_y are found using voltage's calculator to be applied on helicopter systems (Equations 1 and 2).

4. Optimization algorithm

10.22060/EEJ.2026.25565.5962

The Flower Pollination Algorithm (FPA) is a nature-inspired optimization technique based on the pollination process of flowering plants. It mimics the behavior of cross-pollination (global search) and self-pollination (local search) to solve complex optimization problems efficiently. The evaluation of each candidate solution is performed using a nonlinear Simulink model of the 2-DOF helicopter system, which significantly increases the computational cost of the optimization process. Eventually, the algorithm converges to the optimal solution.

The objective function to be minimized is defined as the sum of the squared tracking errors of the pitch and yaw angles.

$$IS\xi = \int_0^T {\xi_p}^2 + {\xi_y}^2 \, dt \tag{30}$$

Where:

$IS\xi$: Integral Squared Error.

ξ_p: Error between desired pitch and helicopter’s pitch.

ξ_y: Error between desired yaw and helicopter’s yaw.

The Integral Squared Error (ISE) criterion is selected as the objective function due to its strong sensitivity to large tracking errors, which is particularly suitable for nonlinear control systems requiring fast convergence. Compared to other performance indices such as Integral Absolute Error (IAE) and Integral Time-weighted Absolute Error (ITAE), ISE provides a more effective penalization of peak errors, making it appropriate for transient performance optimization in the proposed controller design.

The algorithm is used to determine the optimal controller gains by minimizing the selected objective function [23].

Table 2. FPA Parameters

10.22060/EEJ.2026.25565.5962

Parameter	Symbol
Population size (N)	50
Iterations (T)	30
Switching probability (p)	0.03
Scaling factor (c)	0.5
Objective function	$IS\xi$
Control gains	$[k1, k2, k3, k4]$
Bounds	[1, 25]

Table 2 summarizes the main parameters of the Flower Pollination Algorithm used in this work for optimizing the controller gains.

The output vector of the optimization algorithm is given as follow:

$$[k_1 \quad k_2 \quad k_3 \quad k_4] \tag{31}$$

10.22060/EEJ.2026.25565.5962

Initialize parameters: population size N, iterations T, switching probability p, scaling factor c
Define search space bounds for controller gains k_1, k_2, k_3, k_4
Randomly initialize population $x_i = [k_1, k_2, k_3, k_4]$
for each individual $i = 1 \dots N$ **do**
    Run simulation model
    Compute objective function:
    $J_i = \int_0^T (\xi_p^2 + \xi_y^2)\, dt$
end for
Identify global best solution x_g
for iteration $t = 1 \dots T$ **do**
    for each individual $i = 1 \dots N$ **do**
        Generate random number r
        if $r < p$ **then**
            Global pollination:
            $x_i = x_g + c \cdot \text{Levy}(x_i - x_g)$
        else
            Local pollination:
            Select x_j, x_k randomly
            $x_i = x_g + c \cdot (x_j - x_k)$
        end if
        Enforce boundary constraints
        Run simulation model
        Compute J_i
        if $J_i < J_{best}$ **then**
            Update best solution $x_g = x_i$
        end if
    end for
end for
Output: optimal gains $[k_1, k_2, k_3, k_4]$

Fig. 4. FPA based backstepping pseudo code

Figure 4 presents the flowchart of the Flower Pollination Algorithm (FPA) applied for the optimization of the backstepping controller gains. The algorithm starts by initializing a population of candidate solutions within the predefined search space. Each candidate represents a possible set of controller gains, which are evaluated using the MATLAB/Simulink model of the Quanser helicopter through the Integral Squared Error (ISE) performance index. Based on the fitness evaluation, the algorithm updates the population using global and local pollination mechanisms to balance exploration and exploitation. This iterative process continues until the maximum number of iterations is reached, and the best solution is selected as the optimal controller gains.

The algorithm updates candidate solutions using global and local pollination operators. The best solution is selected based on a greedy strategy minimizing the ISE objective function. The convergence behavior exhibits a monotonic decrease until stabilization [24].

5. Results and discussion

The parameters included in the mathematical model are given by the robot manufacturer for use in the development of the controller and the simulation (Table 3).

Table 3. Quanser's 2DOF Helicopter Parameters

Parameter	Symbol	Value
Viscous friction coefficient of Pitch	D_{pp}	0.0071 N/V
Viscous friction coefficient of Yaw	D_{yy}	0.022 N/V
Pitch axis moment of inertia	I_{pp}	0.0215 Kg/m^2
Yaw axis moment of inertia	I_{yy}	0.0237 Kg/m^2
Gravitational acceleration	g	9.8 m/s^2
Length between the fixing point of the body frame and the center of mass	L	0.002 m
Body's weight	m	1.075 Kg
Torque thrust gain	k_{pp}	0.022 Nm/V
Torque thrust gain	k_{yy}	0.0022 Nm/V
Torque thrust gain	k_{py}	0.0221 Nm/V
Torque thrust gain	k_{yp}	-0.0227 Nm/V

After several optimization runs, the optimized backstepping gains were obtained and are presented in Table 4.

Table 4. Obtained controller gains

Angle	Gain 1	Gain 2
Pitch θ	$k1 = 4.2$	$k2 = 24.6$
Yaw ψ	$k3 = 2.28$	$k4 = 10.8$

10.22060/EEJ.2026.25565.5962

First, the step response results are discussed for the two angular positions taking into consideration the motor saturation constraints.

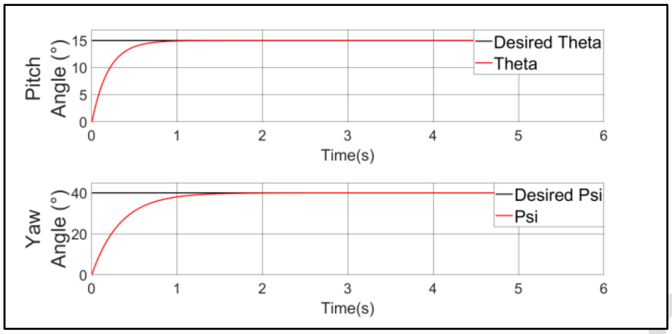

Fig. 4. Pitch and yaw step responses

Figure 4 presents the step responses of pitch angle to a desired input $\theta_d = 15^{\circ}$ and of yaw angle to a desired input $\psi_d = 40^{\circ}$. The results demonstrate the stability of the closed-loop system as well as excellent tracking accuracy and fast transient response. (Table 5).

Table 5. System performances

Angle	Settling time	Overshoot	Steady Error
Pitch θ	$= 0.9$ s	$= 0$ %	$\approx 0.02°$
Yaw ψ	$= 1.4$ s	$= 0$ %	$\approx 0.007°$

Figure 5 presents the control voltages applied to the pitch and yaw motors, together with the corresponding tracking errors (Figure 5).

10.22060/EEJ.2026.25565.5962

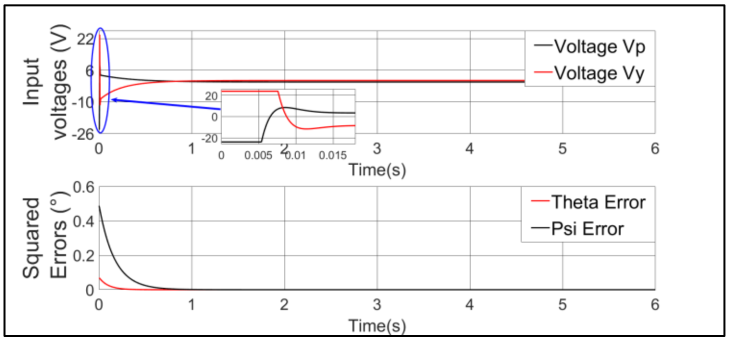

Fig. 5. Input voltages and squared errors of pitch and yaw step responses

The voltages applied by the controller to the pitch and yaw motors remain within the nominal operating range of [-24v +24v] during the helicopter motion. A brief saturation period of less than 8 ms is observed at the beginning of the maneuver, which can be attributed to the maximum utilization of the motors to rapidly reach the desired pitch and yaw positions.

Actuator saturation is considered in the simulation through hard constraints imposed on the input voltages V_p and V_y, which are limited to the physical operating range of the Quanser motors (±24 V). This saturation is implemented inside the Simulink model using nonlinear saturation blocks applied directly to the control signals. Although saturation introduces nonlinear effects that may affect transient performance, the proposed backstepping controller maintains stability due to the Lyapunov-based design and the bounded nature of the control inputs.

According to the second curve of figure 5, the tracking errors of both degrees of freedom (yaw and pitch) quickly converge to a value of $\approx 0°$ in a time of ≈ 0.8 s.

After takeoff, different movement scenarios are simulated to evaluate the controller performance without and with external disturbance.

To further support the claimed contribution of this work, the effectiveness of the proposed Lyapunov-based backstepping controller tuned via the Flower Pollination Algorithm is evaluated under different operating scenarios including step tracking, sinusoidal tracking, and square trajectory tracking. In all cases, the controller demonstrates fast convergence, negligible steady-state error, and strong robustness against nonlinear coupling effects between pitch and yaw dynamics. Unlike conventional fixed-gain backstepping controllers, the optimized gains obtained through FPA allow a better trade-off between transient response and control effort, which is particularly evident under actuator saturation and external disturbance conditions. These results confirm the advantage of combining nonlinear control design with evolutionary optimization in improving overall system performance.

To evaluate the performance of the proposed control strategy and highlight its advantages over conventional approaches, a comparative analysis with commonly used control methods is presented. This comparison considers key aspects such as control structure, optimization technique, robustness to disturbances, actuator saturation handling, and tracking performance. The objective is to provide a clear qualitative assessment of how the proposed method improves upon existing control strategies in the context of nonlinear helicopter systems.

Table 6. Comparative Analysis of Control Strategies for Trajectory Tracking Performance

Method	Control Strategy	Optimization	Saturation Handling	Disturbance Robustness	Tracking Performance
PID	Linear	None	No	Low	Medium
Classical Backstepping	Nonlinear	Manual tuning	Partial	Medium	Good
LQR	Optimal linear	Riccati	No	Medium	Good
Proposed Method	Backstepping + FPA	FPA	Yes	High	Excellent

From Table 6, it can be observed that the proposed method outperforms classical PID, LQR, and conventional backstepping approaches in terms of robustness, tracking accuracy, and the ability to handle nonlinear effects such as actuator saturation and external disturbances. This confirms the effectiveness of the proposed control strategy, which combines Lyapunov-based backstepping with the Flower Pollination Algorithm (FPA) for optimal controller gain tuning.

Scenario 1:

In this scenario, the helicopter maintains a constant elevation angle, ensuring stable pitch behavior during the maneuver. At the same time, the yaw motion follows a smooth periodic oscillation, producing a regular lateral sweeping movement around the central position.

So desired angular positions producing this movement are as follows:

$$\theta_d = 20^{\circ} \tag{32}$$

$$\psi_d = [40.\sin(0.08.t)]^{\circ} \tag{33}$$

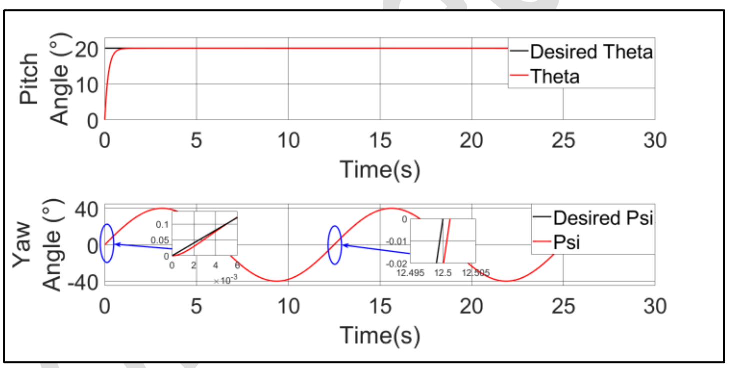

Fig. 6. Pitch step response and yaw sinusoidal tracking

A fixed pitch angular position (20°) is applied as the desired value to ensure forward movement at a fixed speed with a desired sinusoidal trajectory for the yaw angle ψ (helicopter's orientation).

The desired trajectory of the yaw angle ψ is accurately tracked by the helicopter with almost zero position error, demonstrating the effectiveness of the proposed controller, especially since the pitch angle θ is not disturbed during the variation of the orientation angle yaw ψ (Figure 6).

Scenario 2:

The helicopter maintains a slightly lower elevation angle, providing steady pitch control throughout the maneuver. Meanwhile, the yaw motion follows a piecewise-step pattern, generating discrete lateral movements at specific time intervals to simulate abrupt directional changes.

Desired inputs of this scenario are as follows:

$$\theta_d = 10^{\circ} \tag{34}$$

$$\psi_d = \begin{cases} 0^{\circ}, & 0\text{s} < \text{time} < 8\text{s} \\ -10^{\circ}, & 8\text{s} < \text{time} < 16\text{s} \\ -5^{\circ}, & 16\text{s} < \text{time} < 24\text{s} \\ 10^{\circ}, & 24\text{s} < \text{time} < 32\text{s} \\ -20^{\circ}, & 32\text{s} < \text{time} < 40\text{s} \end{cases} \tag{35}$$

This scenario is intended to evaluate the responsiveness of the system during obstacle-avoidance manoeuvres by changing the orientation angle ψ, then a square signal from equation (35) is applied as the desired value of the yaw angle ψ to evaluate the tracking performance of a this variable angular position.

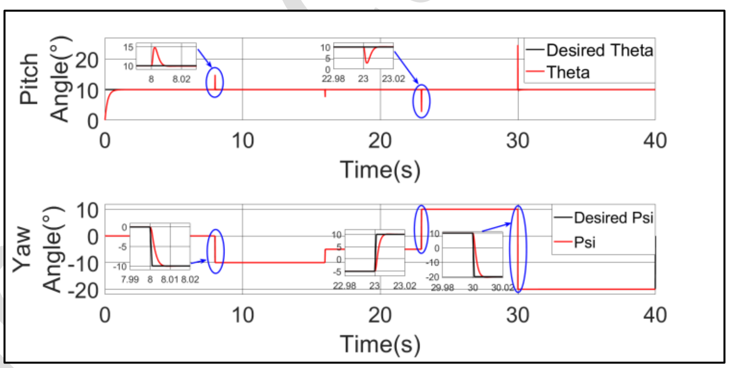

Fig. 7. Pitch step response and yaw square tracking

It is clear from figure 7 that the helicopter tracks the desired trajectory of yaw angle ψ accurately, quickly and without overshoot.

In each of the instants (8s, 16s, 23s and 30s), a small deviation in the pitch angle can be observed because of the coupling in the nonlinear mathematical model of the controlled robot between the angular

10.22060/EEJ.2026.25565.5962

acceleration $\ddot{\theta}$ and $\ddot{\psi}$ (Equations 1 and 2), but it has no influence because it disappears rapidly within approximately 10 and 20 ms.

Scenario 3:

In this scenario, the helicopter maintains a constant elevation angle, ensuring stable pitch behavior throughout the maneuver. Simultaneously, the yaw motion follows a smooth periodic oscillation, producing a regular lateral sweeping movement, while external disturbances are applied after 20 seconds on both pitch and yaw channels to evaluate the system's robustness.

Desired inputs are the following:

$$\theta_d = 20^{\circ} \tag{36}$$

$$\psi_d = [40. sin(0.08. t)]^{\circ} \tag{37}$$

The disturbance signals are defined as follows:

$$\delta_p = \begin{matrix} random\,, & 0s < time \leq 20s \\ 0\,v\,, & 20s < time \leq 40s \end{matrix} \tag{38}$$

$$\delta_y = \begin{matrix} random\,, & 0s < time \leq 20s \\ 0\,v\,, & 20s < time \leq 40s \end{matrix} \tag{39}$$

The external disturbance signals are modeled as bounded random inputs to represent unmodeled dynamics, aerodynamic effects, and external environmental perturbations such as airflow variations. This type of disturbance is commonly used in nonlinear control validation studies to evaluate robustness under uncertain operating conditions. After 20 seconds, the disturbances are removed to assess the system's ability to recover and converge back to the desired trajectories.

External disturbances are simulated by adding the bounded voltage signals δ_p and δ_y to the control voltages V_p and V_y. This approach emulates the effect of external forces and modeling uncertainties acting on the helicopter during flight, thereby providing a realistic framework for robustness evaluation (Figure 8).

10.22060/EEJ.2026.25565.5962

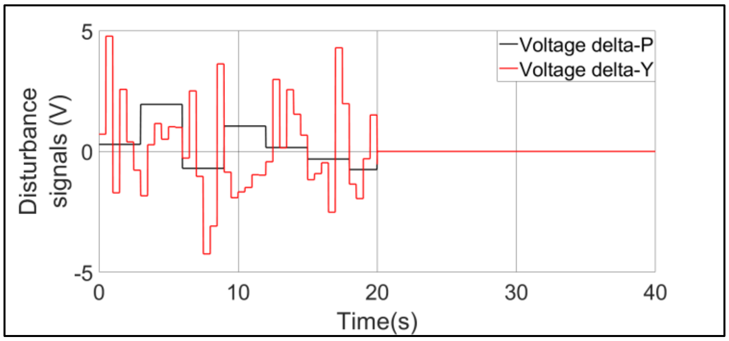

Fig. 8. Disturbance signals applied to the system

A variable square signal is applied as the desired pitch angle θ which will create a variation in the forward movement speed of the helicopter and external disturbing forces are applied to the helicopter at different times of the scenario to check the robustness of the system.

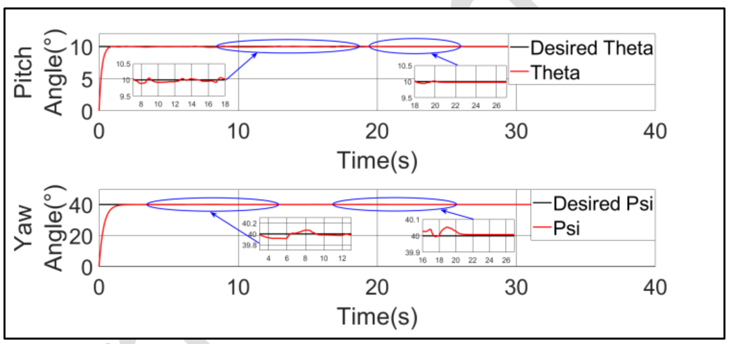

Fig. 9. Pitch and yaw responses under disturbance

In this scenario, the robustness of the system against external disturbances is clearly demonstrated. It can be observed that, when disturbances are applied, the pitch and yaw responses remain stable and quickly return to the desired trajectory after the 20th second, when the disturbance is removed (Figures 8 and 9). Overall, the results obtained in all scenarios demonstrate the effectiveness of the proposed controller. The helicopter reaches the desired angular positions with fast convergence, high tracking accuracy, and negligible steady-state error while respecting actuator saturation limits. In 2nd scenario, small transient deviations appear due to the nonlinear coupling between the pitch and yaw dynamics; however, their amplitudes remain very small and they disappear rapidly. Furthermore, the results obtained under external

10.22060/EEJ.2026.25565.5962

disturbances confirm the robustness of the proposed control strategy and its ability to maintain stable tracking performance in the presence of uncertainties.

Although the proposed method is not directly compared with other advanced nonlinear controllers in this study, the performance can be qualitatively assessed through benchmark characteristics such as fast settling time, zero steady-state error, and robustness under disturbance and saturation constraints, as demonstrated across all simulation scenarios.

Conclusion:

This paper proposes a nonlinear backstepping controller of a 2DOF Quanser helicopter optimized by the Flower Pollination Algorithm FPA. The nonlinear model of the helicopter is presented, and a backstepping controller is developed based on Lyapunov stability theory. The controller gains are subsequently optimized using the Flower Pollination Algorithm. The results, which are: step responses and examples of simulated helicopter movement scenarios show that the proposed control method is very efficient in terms of stability, precision and speed compared with other control approaches reported in the literature for this type of aerial system and also the disturbance-rejection tests demonstrate the robustness of the controlled system while taking into consideration the saturation limit of the actuator motors of the controlled robot which demonstrates the practical feasibility of the proposed control strategy.

References

[1] B.M. Kim, S.J. Yoo, Approximation-Based Quantized State Feedback Tracking of Uncertain Input-Saturated MIMO Nonlinear Systems with Application to 2-DOF Helicopter, Mathematics, 9(9) (2021) 1062.
[2] B. Wu, J. Wu, W. He, G. Tang, Z. Zhao, Adaptive Neural Control for an Uncertain 2-DOF Helicopter System with Unknown Control Direction and Actuator Faults, Mathematics, 10(22) (2022) 4342.
[3] J.M. Mendel, Type-2 fuzzy sets, in: Uncertain Rule-Based Fuzzy Systems: Introduction and New Directions, 2nd Edition, Springer, 2017, pp. 259-306.
[4] N. Rouis, I. N'Doye, T.-M. Laleg-Kirati, Model-free LQR based PID controller for trajectory tracking of 2-DoF helicopter: comparison and experimental results, arXiv preprint arXiv:2103.10988, (2021).
[5] B. Wu, J. Wu, J. Zhang, G. Tang, Z. Zhao, Adaptive neural control of a 2DOF helicopter with input saturation and time-varying output constraint, in: Actuators, MDPI, 2022, pp. 336.

10.22060/EEJ.2026.25565.5962

[6] O.Y. Ismael, M.N. Noaman, I.K. Abdullah, Fick's Law Algorithm Based-Nonlinear Model Predictive Control of Twin Rotor MIMO System, Journal of Robotics and Control (JRC), 5(3) (2024) 694-705.
[7] M. Reyhanoglu, M. Jafari, M. Rehan, Simple learning-based robust trajectory tracking control of a 2-DOF helicopter system, Electronics, 11(13) (2022) 2075.
[8] J. Sivadasan, J.R.J. Shiney, Modified nondominated sorting genetic algorithm-based multiobjective optimization of a cross-coupled nonlinear PID controller for a Twin Rotor System, Journal of Engineering and Applied Science, 70(1) (2023) 133.
[9] A. Rezoug, A. Messah, W.A. Messaoud, K. Baizid, J. Iqbal, Adaptive-optimal MIMO nonsingular terminal sliding mode control of twin-rotor helicopter system: meta-heuristics and super-twisting based control approach, Journal of the Brazilian Society of Mechanical Sciences and Engineering, 46(3) (2024) 162.
[10] T.-D. Huynh, N.-T. Bach, Q.-D. Le, D.-D. Le, V.-H. Bui, H.-A. Vo, V.-N.-L. Nguyen, P.-H. Pham, H.-D. Nguyen, V.-D.-H. Nguyen, Implementation of fuzzy-PID controller for 2-DOF helicopter, Journal of Fuzzy Systems and Control, 2(2) (2024) 74-80.
[11] S. Haider, S. Ali, A. Rasool, A.B. Huda, Experimental Validation of State Estimation of Non-Linear Twin Rotor System using Extended Kalman Filter, Pakistan Journal of Engineering and Applied Sciences, (2023).
[12] M. Ahmad, F. Azeem, H.A. Zidan, Robust residual generator design for sensor fault detection in twin rotor aerodynamic system, e-Prime-Advances in Electrical Engineering, Electronics and Energy, 8 (2024) 100620.
[13] Y. Martinez-Armero, J.B. Renteria-Mena, E. Giraldo, Robust Embedded Control applied to a Twin Rotor MIMO System, Engineering Letters, 31(1) (2023).
[14] M.C. Maya-Rodriguez, M.A. López-Pacheco, Y. Lozano-Hernández, V.G. Sánchez-Meza, L.A. Cantera-Cantera, R. Tolentino-Eslava, Integration of cnn in a dynamic model-based controller for control of a 2dof helicopter with tail rotor perturbations, IEEE Access, 10 (2022) 73474-73483.
[15] N. Abbas, X. Liu, J. Iqbal, Robust GDI-based adaptive recursive sliding mode control (RGDI-ARSMC) for a highly nonlinear MIMO system with varying dynamics of UAV, Journal of Mechanical Science and Technology, 38(4) (2024) 2015-2028.
[16] A. Haruna, Z. Mohamed, A.M. Abdullahi, M.A.M. Basri, A review of control algorithms for twin rotor systems, Applications of Modelling and Simulation, 7 (2023) 93-99.
[17] M.A. Zuñiga, L.A. Ramírez, G. Romero, E. Alcorta-García, A. Arceo, Passive fault-tolerant control of a 2-dof robotic helicopter, Information, 12(11) (2021) 445.
[18] S.I. Abdelmaksoud, M. Mailah, A.M. Abdallah, Practical real-time implementation of a disturbance rejection control scheme for a twin-rotor helicopter system using intelligent active force control, Ieee Access, 9 (2020) 4886-4901.
[19] N. Abbas, X. Pan, A. Raheem, R. Shakoor, Z.A. Arfeen, M. Rashid, F. Umer, N. Safdar, X. Liu, Real-time robust generalized dynamic inversion based optimization control for coupled twin rotor MIMO system, Scientific Reports, 12(1) (2022) 17852.
[20] N. Abbas, X. Liu, J. Iqbal, A flexible mixed-optimization with H∞ control for coupled twin rotor MIMO system based on the method of inequality (MOI)-An experimental study, Plos one, 19(3) (2024) e0300305.
[21] Sajjadi, S., Mehrandezh, M., & Janabi-Sharifi, F. (2022). A Cascaded and Adaptive Visual Predictive Control Approach for Real-Time Dynamic Visual Servoing. *Drones*, *6*(5), 127. https://doi.org/10.3390/drones6050127
[22] N. Abbas, Z. Abbas, X. Liu, Adaptive recursive sliding mode control (ARSMC)-Based UAV control for future smart cities, Applied Sciences, 13(11) (2023) 6790.

10.22060/EEJ.2026.25565.5962

[23] I.B. Ghiloubi, L. Abdou, O. Lahmar, Adjusted linear quadratic regulator-proportional-derivative control of Quanser's three degrees of freedom helicopter based on flower pollination algorithm under external disturbances, IAES International Journal of Robotics and Automation (IJRA), 13(4) (2024) 432-444.
[24] I.B. Ghiloubi, L. Abdou, O. Lahmar, Anti-Collision Formation Control for Drone Swarms Tracking Aerial Targets Under Wind Disturbance, International Journal of Robotics and Control Systems, 5(6) (2025) 2831-2852.